Soft Matter

Accepted Manuscript

This is an *Accepted Manuscript*, which has been through the Royal Society of Chemistry peer review process and has been accepted for publication.

Accepted Manuscripts are published online shortly after acceptance, before technical editing, formatting and proof reading. Using this free service, authors can make their results available to the community, in citable form, before we publish the edited article. We will replace this *Accepted Manuscript* with the edited and formatted *Advance Article* as soon as it is available.

You can find more information about *Accepted Manuscripts* in the Information for Authors.

Please note that technical editing may introduce minor changes to the text and/or graphics, which may alter content. The journal's standard Terms & Conditions and the Ethical guidelines still apply. In no event shall the Royal Society of Chemistry be held responsible for any errors or omissions in this *Accepted Manuscript* or any consequences arising from the use of any information it contains.

ROYAL SOCIETY OF CHEMISTRY

www.rsc.org/softmatter

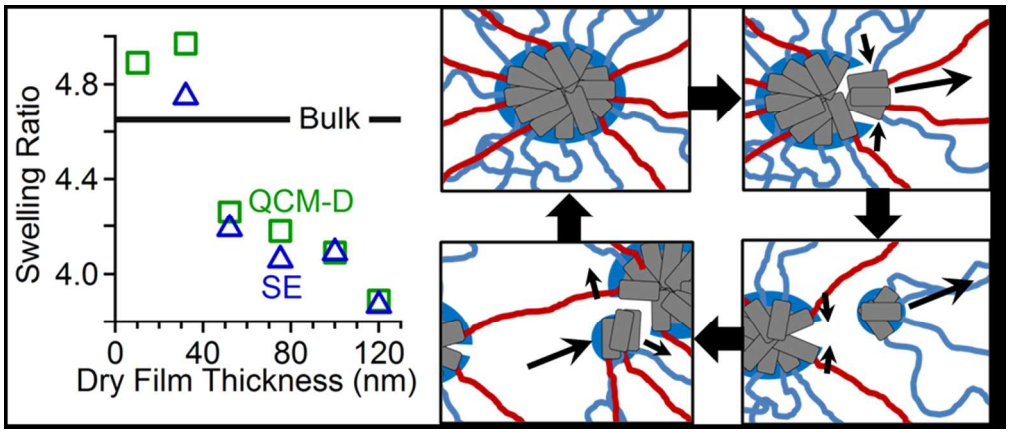

Re-arrangement of supramolecular physical crosslinks enables near bulk-like swelling
170x71mm (150 x 150 DPI)

Soft Matter Accepted Manuscript

Soft Matter

RSCPublishing

ARTICLE

Overcoming confinement limited swelling in hydrogel thin films using supramolecular interactions

Cite this: DOI: 10.1039/xoxxoooooox

Received ooth January 2012,
Accepted ooth January 2012

DOI: 10.1039/xoxxoooooox

www.rsc.org/

Clinton G. Wiener, R. A. Weiss and Bryan D. Vogt*

The thin film behavior of poly(N-isopropylacrylamide-*stat*-2-(N-ethylperfluorooctane sulfonamido)ethyl acrylate) (NIPAAm-*stat*-FOSA) based hydrogels containing 5 mol% FOSA was elucidated using quartz crystal microbalance with dissipation (QCM-D) in combination with spectroscopic ellipsometry (SE) through examination of the lower critical solution temperature (LCST) and temperature dependent swelling ratio over (dry) thicknesses ranging from 10 nm to 121 nm. For all thin films measured, the LCST was shown to increase (> 3 ºC) in comparison to that of the bulk sample. However for these films, the increase in LCST was statistically identical, irrespective of thickness. Surprisingly, the volumetric swelling of the hydrogel in thin films, even at temperatures less than the LCST, was similar (within 20 %) to the volumetric swelling of the bulk hydrogel, despite the expected significant decrease associated with the hydrogel being constrained by the substrate as predicted by one dimensional Flory-Rehner theory. We attribute this enhancement in swelling compared to theoretical expectations to the ability of the hydrophobic crosslinks to re-arrange under stress, which provides a mechanism to alleviate the decreased dimensionality caused by the substrate; this mechanism is consistent with a large hysteresis in the swelling when cycling between 30 ºC and 5 ºC. Unlike the LCST, the swelling ratio increases with decreasing film thickness. At low temperatures (below the LCST), the volume swelling ratio increased from 3.9 to 4.9, while at temperatures above the LCST the swelling ratio increased from 1.5 to 2.5 when the film thickness decreased from 121 nm to 10 nm. The combination of facile processing through solution casting without the need for additional crosslinking chemistry and limited thickness dependent variation of swelling and LCST behavior in these physically crosslinked hydrogels makes these materials attractive for applications requiring thermoresponsive soft coatings.

Introduction

The diverse chemistries available for the fabrication of hydrogel materials provides a pathway to tune their physical properties to enable utilization in a variety of applications, including drug delivery,[1, 2] tissue scaffolds,[3] sensors,[1, 4] cell immobilization,[5] control of flow in channels,[6, 7] biomedical devices[8] and soft machines.[9] In many of these applications, the hydrogel is constrained to dimensions from the micrometer to nanometer scales, commonly as microparticles or thin film coatings. By inclusion of responsive groups in the chemistry of the hydrogel, such as polyacrylamide (PAAM)/poly(acrylic acid) (PAAC)[10] or poly(N-isopropyl acrylamide) (PNIPAAm)[11, 12], the particles or coatings can exhibit tunable properties that promote a response to environmental stimuli, e.g., the rise in local temperature in a tumor to trigger drug release[13]. Thermally responsive hydrogels, PNIPAAm in particular, have been extensively studied in the bulk,[14-16] microparticles,[17] and thin coatings[18]. The thermoresponsive behavior of PNIPAAm is resultant from its lower critical solution temperature (LCST) and the associated differences in the swelling above and below this phase transition. However, the swelling behavior can be significantly different in thin films as compared to the bulk hydrogel. Thus, the thin film properties of these hydrogels are important to ensure performance and operation requirements for applications are still met.

To generate thin PNIPAAm coatings, two strategies are commonly used: grafting a brush to the surface[19-21] or *in-situ* chemical crosslinking using a thin coating.[1, 22, 23] For brushes, the LCST can be dramatically shifted depending on the graft density.[21] The thickness of these brush layers is controlled by the graft density and the molecular weight of the grafted chain. These properties also impact the relative difference in thickness between the collapsed (high temperature) and swollen (low temperature) states of the brush.[19]

Soft Matter Accepted Manuscript

Conversely, thin (ca. 150 nm dry) hydrogel films can be formed by crosslinking PNIPAAm on a substrate of interest. Such films generally exhibit an LCST that is 2-4 ºC greater than the LCST of the analogous bulk hydrogel (defined as a free standing film at least 0.5 mm thick with the same chemical composition and crosslink density).[1, 22, 23] This effect on the LCST for chemically crosslinked films is less than typically observed for PNIPAAm brushes. However unlike the LCST, the swelling of thin chemically crosslinked PNIPAAm films is significantly reduced as compared to the bulk. For example, Harmon et al.[24] observed a 100-fold increase in volume upon swelling of bulk covalently crosslinked PNIPAAm, but a thin constrained film exhibited only a 15 fold-increase in volume upon swelling. This significant decrease in the volumetric response of the hydrogel network can significantly alter their properties in thin films.

These differences between the thin film and bulk properties of hydrogels are generally attributed to the constraints in swelling by the substrate. For a thin film, if the hydrogel is not well adhered to the substrate, osmotic stresses associated with swelling will delaminate the film. The adhesion to the substrate limits the deformation of the hydrogel such that the volumetric change is almost exclusively unidirectional through the thickness of the film. For one dimensional (1D), constrained swelling of a crosslinked polymer,[25] Flory-Rehner theory[26] predicts that ideal volumetric swelling ratio for a constrained network should be the square root of the isotropic bulk volumetric swelling ratio of the unconstrained network. 1D constrained swelling infers that the thickness swelling ratio is indistinguishable from the volumetric swelling ratio. For chemically crosslinked poly(dimethylacrylamide) hydrogels covering a wide range of crosslink density, Toomey, et al. found good agreement between the predicted constrained thin film swelling and experimental results.[25]

Additionally, component segregation to interfaces[27] during synthesis of crosslinked PNIPAAM thin films[22] can lead to non-uniform crosslink density through the film thickness. Moreover, the chain conformation may be altered due to confinement effects[28] and those conformations may be locked-in by the crosslinking reaction carried out in the dry state of the thin films. For polystyrene thin films, Napolitano and Wubbenhorst reported that chains were compressed to produce a pancake-like conformation,[28] and a similar anisotropy may be present in thin PNIPAAm films. That would impact the distribution of crosslinks and the conformations available to the chain upon swelling, since the covalent crosslinks are chemically fixed and cannot rearrange.

A facile method to enable rearrangement of the network crosslinks is to use physical crosslinks. In that case, the crosslinks can dissociate as a mechano-response to the stresses generated from swelling, which allows the chains to rearrange if the osmotic stress is sufficiently large. Once the stresses are relaxed, however, the broken physical crosslinks reform to restore the network, with a similar crosslink density as the initial gel network.

One such thermally responsive, physically crosslinked hydrogel, consists of a random copolymer of NIPAAm and 2-(N-ethylperfluorooctanesulfonamido)ethyl acrylate (FOSA).[14] The hydrophobic FOSA aggregates into nanodomains that are dispersed in a continuous poly(NIPAAm) phase, and the nanodomains behave as supramolecular crosslinks. The fluorocarbon chain in the FOSA produces stronger hydrophobic associations than typically provided by a hydrocarbon chain in other hydrophobically-modified hydrogels.[29] NIPAAm-FOSA copolymers can form gels in water at FOSA concentrations in the copolymer as low as 2 mol%.[16] Similar physical hydrogels based on N,N'-dimethyl acrylamide (DMA) and FOSA copolymers exhibit strength and toughness[15] similar to the '*double networks'* hydrogels.[27] The toughness of those physical hydrogels was attributed to the responsive character of the hydrophobic associations to stress,[15] which allows the nanodomains to rearrange and reform in response to an applied load. In light of these observations, the motivation for the research reported herein was that physically crosslinked hydrogels may provide a means to overcome the constraints from the substrate on the swelling of thin film hydrogels.

This paper describes the temperature-dependent swelling behavior of NIPAAm-FOSA copolymers containing 5 mol% FOSA, denoted as NF5, for a wide range of film thicknesses using a combination of spectroscopic ellipsometry (SE) and quartz crystal micro-balance with dissipation (QCM-D). These measurements provide complementary information as the SE measurements are challenged in the thin film limit by the coupling of refractive index and thickness,[30] while for thicker hydrogels, the QCM-D response is strongly influenced by the viscoelastic nature of the film.[25] This necessitates recursive modeling and significant assumptions regarding the frequency dependence of the viscoelastic properties.[31] In contrast to chemically crosslinked PNIPAAm, where confinement effects produced over 50% reduction in thin film swelling,[25] the volumetric swelling of the physically crosslinked hydrogel thin films was within 20 % of the bulk.

Experimental

Materials. The synthesis of the NF5 copolymer by a free-radical copolymerization of NIPAAm and FOSA has been previously described[14,16]. The same copolymer (NF5) sample that was used in ref (14) was used in this work. The characteristics of the copolymer were M_w = 6.4 x 10^4 Da, M_n = 3.4 x 10^4 Da and 5 mol % FOSA.[14] Toluene (99.8 %, ACS Grade), isopropyl alcohol (99.5%, ACS Grade), and 1,4-dioxane (99.8%, ACS Grade) were purchased from Sigma Aldrich and used as received for preparation of the thin films. Deionized water (~ 1-5 ppm inorganic) was used in all the swelling experiments.

Sample preparation and measurement baseline. Quartz sensors (QSX-335, Q-Sense) with successive layers of titanium, titanium oxide, and silica oxide deposited on a standard gold quartz sensor were used as film substrates for all measurements. All sensors were cleaned prior to use by sonication in toluene,

Soft Matter Accepted Manuscript

 This journal is © The Royal Society of Chemistry 2012

then isopropanol and finally deionized (DI) water. The sensor was then rinsed thoroughly with DI water and blown dry with nitrogen. Prior to coating with the NF5, the optical properties of the bare sensors were determined using a spectroscopic ellipsometer (SE) (*JA Woollam M-2000UI*) and the baseline impedance of the quartz sensor was determined in air and in DI water at 25 ºC using the quartz crystal microbalance with dissipation (QCM-D) (*Model E1*, *Q-Sense*). The sensors were again rinsed with DI water, blown dry with nitrogen and then further cleaned with ultraviolet ozone (UVO) (*UVO CLEANER®, Model 42, Jelight Company Inc.*) for 90 s.

Immediately following the UVO exposure, the NF5 was spin-cast onto the sensor from a 1,4-dioxane solution at 2500 rpm for 30 seconds. After coating, the sensors were annealed at 150 ºC for at least 18 hours to aid in solvent removal, ensure that the film was completely dry, and promote the self-assembly of the FOSA nanodomains. Upon removal from the oven, the sensors were immediately placed in a desiccator under vacuum to ensure the samples remained free of water. The initial dry coating thickness was determined in air using SE to obtain a reasonable optical model for the stack on the quartz sensor using the methodology described by Richter and co-workers.[32]

Characterization of swelling. Simultaneous measurements of SE and QCM-D were performed using a combined QCM-D/SE cell (*Q-Sense, Ellipsometry Module*). This system allows QCM-D measurement of quartz sensors in fluid and simultaneous SE measurement through BK7 glass windows with the beam incident on the sensor surface at 65°. For the SE measurements, wavelengths below 400 nm were not included due to a slight absorbance at these lower wavelengths by the BK7 windows.

The QCM-D was used to measure the mass adhered to the sensor surface (which enables the calculation of film thickness, if the density is known, herein a density of 1 g/cm^3 was assumed for the film) and its viscoelastic properties[33]. The latter determination is based on the oscillation frequency of the driven quartz, F, and the rate of decay of the oscillation amplitude, which is directly related to the dissipation, D[34], when the potential is removed. Prior to filling the cell with DI water, the sensor was measured in air for 10 min to provide a stable baseline. The cell was then flushed with DI water for 10 min at 100 µL/min, with the water pulled in using a 2 channel peristaltic pump. All ports were checked to insure removal of air. Subsequently, the flow of DI water was reduced to 50 µL/min for at least 40 min at 25 ºC until a frequency change of less than 6 Hz/hr was obtained.

The fundamental frequency and overtones (1-13, odd only) from the QCM-D were again determined using a full frequency scan in order to correct for any perturbation that occurred due to the viscous loading of the QCM-D sensor by the addition of water. The temperature-dependent swelling of the NF5 coating on the sensors was then determined by heating the cell to 35 ºC, restoring the water flow for 5 min to remove any air bubbles that may have formed during heating, and measuring the swelling under quiescent conditions to minimize the duty cycle demand. The temperature was decreased in 1-2 ºC steps every 60 min until 5 ºC was reached. Typical data collection time for the cooling cycle for each film was 24 h.

Data analysis. QCM-D and SE require recursive modeling to determine the film thickness and physical properties such as viscosity, η, shear modulus, µ, and refractive index associated with the hydrogel. For QCM-D, the difference in F and D between the uncoated and NF5-coated sensor in water at 25 ºC was used to calculate the swelling of the thin films. For assessing the thickness, measurements over the last 20 min at each temperature were fit with the recursive model.[31] The QCM-D data were averaged over 5 s intervals to reduce the effect of noise. System temperature effects, which are unrelated to the hydrogel film, can be significant especially for the thinnest films. These effects include thermal stresses applied to the crystal and the temperature dependence of the resonance frequencies. Prior to fitting the experimental data to the recursive model, the effect of temperature on the system was subtracted from the raw data. A detailed explanation of this temperature correction is outlined in the Electronic Supplemental Information, ESI, (Part 1).

Figure S4 (ESI) illustrates the large error in the resulting thickness calculation if the device and bulk water temperature effects are not removed. From the recursive fit of the frequency (i.e., mass) and the dissipation (viscous loss), the thickness and viscoelastic properties of the hydrogel were determined using an average of the last 20 minutes for each temperature step. The QCM-D data were analyzed using Q-Tools software with a frequency-dependent Voigt model to calculate the viscoelastic properties of the sample from the measured dissipation and frequency change of the sensor.[33,35] The zero baseline for all measurements and temperature corrections was 25 °C.

The temperature corrected QCM-D data were fit with the extended viscoelastic model,[32] which is a frequency-dependent Voigt based viscoelastic model.[31] Due to anomalous behavior at low temperatures associated with a frequency upturn with swelling at higher overtones (ESI Part 5), only the 3rd and 5th overtones were utilized in the fit unless otherwise noted. In order to achieve a reasonable fit, the model parameters were bracketed as: $h_0 < h < 6h_0$, where h_0 was the dry film thickness, $10^5 < \mu < 10^8$ Pa), and $0.01 < \eta < 1$ Pa·s. Once χ^2 was minimized, the modeling was restarted to ensure that the modeling in Q-Tools program could generate the same result globally. The final values were only used and reported herein when they could be reproduced.

The SE thin film data from wavelengths 400 nm to 1150 nm were modeled using a simple Cauchy layer[35] to describe the optical properties of the hydrogel. Temperature dependent optical properties of water were included in fitting of the SE data to increase accuracy of the fits.

To quantify the lower critical solution temperature, LCST, and the breadth of the transition, the temperature dependent thickness as determined from both QCM-D and SE was fit to a sigmoid function, as shown in Equation 1, following the prior reports by Harmon, et al.[24]

Soft Matter Accepted Manuscript

$$\frac{h}{h_0} = \left(\frac{h}{h_0}\right)_{max} + \left[\frac{\left(\frac{h}{h_0}\right)_{collapsed} - \left(\frac{h}{h_0}\right)_{max}}{1+\exp\left(\frac{T_{LCST}-T}{\sigma}\right)}\right] \quad (1)$$

where $(h/h_0)_{collapsed}$ is the swelling ratio at high temperature (e.g., collapsed state), $(h/h_0)_{max}$ is the swelling ratio at low temperature (e.g., highly swollen state), T_{LCST} is the inflection temperature that is defined as the LCST, and σ is the half-width of the sigmoid, which provides a measure of the width of the swelling transition. Details of sigmoid fit and illustration can be found in the ESI (Part 2). It should be noted that in this manuscript that we will use LCST to denote the volumetric swelling transition at atmospheric pressure. Rigorously by definition, the LCST occurs if the isobar passes through the critical point and would require examination of both temperature and pressure as independent variable.[36] However as the volumetric transition at 1 bar is commonly described as the LCST in the hydrogel literature,[37-39] we will utilize this more standard convention.

Results and Discussion

Figure 1 illustrates how the apparent equilibrium volumetric swelling ratio (V/V_0) of NF5 in DI water depends on the film thickness as the hydrogel is cooled through the LCST. The low temperature swelling is very similar to that for the bulk hydrogel. This similarity in swelling is striking given the significant differences reported between thin films and bulk for chemically crosslinked hydrogels.[24] The Flory-Rehner theory for thin constrained films[25] predicts a volumetric swelling ratio of 2.2 at the lowest temperature based on the bulk swelling, but the measured volumetric swelling ratio was greater than 3.9 for all the films examined. When examining the low temperature swelling data more carefully, there was an increase in the volumetric swelling ratio as the film thickness decreases.

Figure 1C illustrates this behavior more clearly with the swelling ratio at 5 °C increasing from 3.9 to 4.9 as the dry NF5 thickness was decreased from 120 nm to 10 nm (for confined films, h/h_0 is indistinguishable from V/V_0). For the thinnest dry film thickness, 10 nm, the short optical path length of the hydrogel and the relatively small difference in refractive index between the hydrogel and water in the highly swollen state resulted in significant uncertainty in the SE fit due to the coupling of refractive index and thickness. As such, those data are not reported. Between 10 nm and 32 nm, there was no further increase in swelling as determined by the QCM-D, so it appears as if the swelling ratio reached a limit. In the thin film limit, the size of the hydrophobic domains (~ 6.4 nm, as measured in bulk[14, 40]) was of the same order as film thickness and thus rearrangement of these hydrophobic domains may be less constrained, which may explain the volumetric swelling ratio being very similar to the bulk.

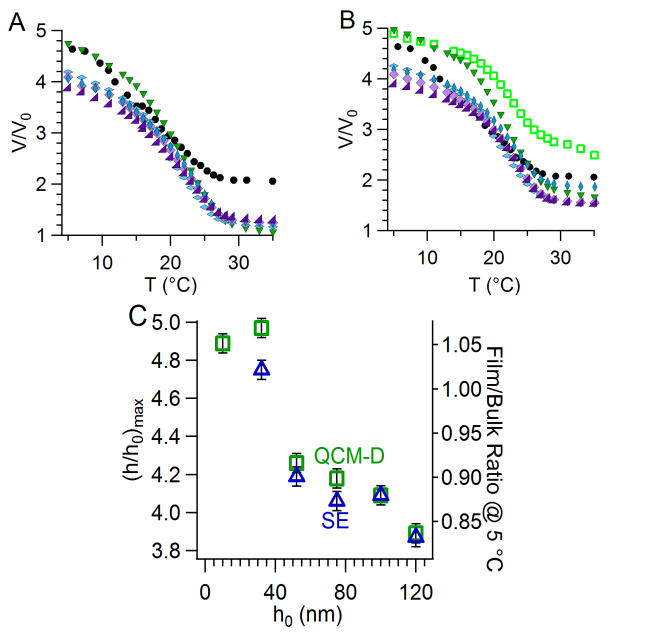

Figure 1. Volumetric swelling ratio (V/V_0) for NF5 thin films equilibrated in water as the temperature is decreased from 35 ˚C to 5 ˚C, determined by SE (**A**) and QCM-D (**B**). NF5 film thicknesses shown are: 10 nm (□), 32 nm (▼), 52 nm (◂▸), 75 nm (♦), 100 nm (◆) and 120 nm (◢). The open symbol 10 nm film was modeled only in QCM-D due to its limited optical path length. Comparison to bulk (●) volumetric swelling measurement is provided as reference. (**C**) Thickness swelling ratios (left axis) from SE (△) and QCM-D (□) at 5 °C and normalized volumetric swelling ratio for the films relative to the bulk hydrogel (right axis).

The swelling of the two thinnest films at 5 °C was actually greater than the bulk hydrogel. That behavior is contradictory to expectations and prior reports for chemically crosslinked PNIPAAm.[24, 25] Although water is known to accumulate at a silica-polymer interface,[41] prior work concluded that a hydrophilic substrate had little effect on the swelling of thin PNIPAAm films.[23] Consistent with the prior work, the swelling of NF5 on SiO_2 and gold coated QCM-D sensors was identical. Nonetheless, the low temperature volumetric swelling ratio was greater than 80% of the bulk for all films examined. Moreover, there was good agreement in the swelling ratio determined by QCM-D and SE measurements confirming that the swelling is not an artifact of the measurement.

At high temperatures ($T > T_{LCST}$), the swelling for the films that were 30 nm (dry) and thicker was significantly less than for the bulk hydrogel. Toomey, et al[25] predicted that the swelling ratio of the film should be the square root of the bulk swelling. Thus, the volumetric swelling ratio should be 1.4 in the collapsed state of the thin films, since the bulk hydrogel swelled to approximately twice its dry volume at the same conditions. That prediction agrees well with measurements for the hydrogel thin films with the volumetric swelling ratio for SE ranging from 1.2 to 1.4 and for that measured by the QCM-D ranging from 1.5 to 1.9 (excluding the 10 nm film).

To explain the consistently greater swelling reported from QCM-D (Figure 1B) than from SE (Figure 1A), the sensitivity of the respective instruments must be considered. The QCM-D

Soft Matter Accepted Manuscript

This journal is © The Royal Society of Chemistry 2012

reporting greater swelling than SE is consistent with prior reports associated with adsorption of proteins to the surface.[42] This difference is attributed to the coupling of bound water to the surface of the adsorbed layer. Only QCM-D, not SE, is sensitive to coupled water[43] at the hydrogel surface. Figure 2 clearly illustrates how the swelling ratio measured by QCM-D is consistently greater than that measured by SE at high temperatures, irrespective of film thickness. The offset between QCM-D and SE was relatively consistent at lower swelling ratios, and that result should be due to the coupled water[43] at the hydrogel surface, to which only the QCM-D is sensitive.

One unusual observation was that the swelling for the thicker films at low temperature showed the QCM-D thickness approaching the thickness measured by SE, which is unexpected based on prior comparisons of optical and acoustic measurements.[42] This behavior is attributed to issues with the QCM-D measurement of these thick, lossy films. Although the films continued to swell at low temperature as determined by SE, the frequency of the higher overtones actually increased, which is typically associated with a loss of mass, which is more thoroughly described in the ESI (Part 5). For the thick films, only the 3rd and 5th overtones were used for determining the thickness from QCM-D, but even these overtones may underreport the frequency (hence, thickness).

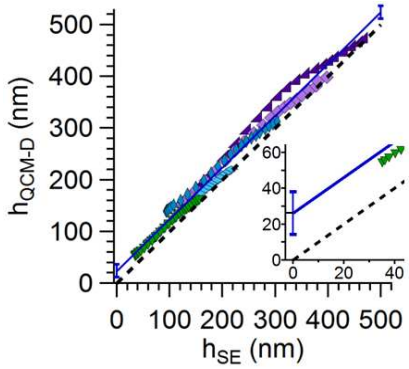

Figure 2. Comparison of hydrogel thickness from QCM-D and SE. For consistency, the thickness from SE and QCM-D should be identical (dashed line). A linear fit of these data before the frequency upturn at high swelling fractions is shown by the solid blue line. This suggests that the average thickness of the coupled water layer associated with QCM-D is 26 ± 12 nm. NF5 film thicknesses shown are: 32 nm (▼), 52 nm (◂▸), 75 nm (♦), 100 nm (◆), and 120 nm (◢).

If one neglects the thickness measurements from QCM-D data where an upturn in frequency was observed at any measured overtone, the average thickness of the coupled water was 26 ± 12 nm for all of the films, as illustrated in Figure 2. At 30 °C, the film thickness calculated from QCM-D was on average 29 nm greater than that measured by SE, and that difference agrees well with the estimated coupled water thickness. However, application of that correction to the data at 5 °C results in significant mismatch between QCM-D and SE. Details of the comparison for each film with and without this coupled water layer are included in ESI (Part 4). For consistency, we have not included this correction to any data included herein outside of the ESI.

With the good agreement in general between SE and QCM-D for the thickness dependent behavior of the NF5 hydrogel films (Figure 1), the utilization of only the 3rd and 5th overtones in the modeling of the QCM-D data does not appear to adversely impact the analysis. To further illustrate the general agreement between QCM-D and SE, Figure 3 illustrates the analysis of the temperature dependent swelling ratio (from Figure 1) using a sigmoid fit (equation 1) to determine T_{LCST} and the width of the transition (2σ). As shown in Figure 3A, an increased T_{LCST} for all of the thin films of 3-5 ºC as compared to the bulk was determined in both SE and QCM-D measurements. There is a discrepancy of approximately 1 ºC in the T_{LCST} between the SE and QCM-D measurements, but this difference is within the uncertainty of the measurement. There is a clear increase of T_{LCST} in the thin films measured as compared to the bulk. A similar increase in T_{LCST} for film thicknesses below 250 nm has also been reported for covalently crosslinked PNIPAAm films,[1, 22, 23] so this behavior is not surprising.

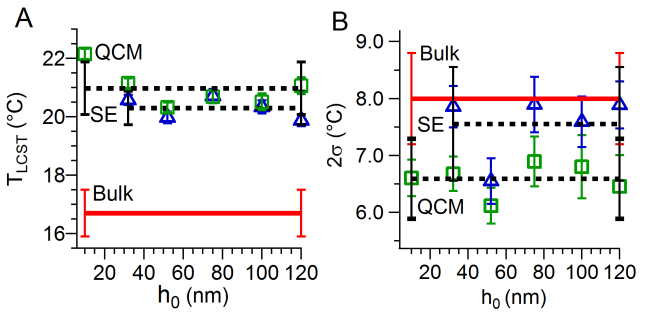

Figure 3. Analysis of the swelling data using equation (1) to determine (**A**) T_{LCST} and (**B**) LCST transition width (2σ) from the QCM-D (□) and SE (△) measurements as a function of film thickness. The dashed lines illustrate the average for each measurement along with the associated standard deviation for each data set. The bulk data (solid red line) is included as a reference.

Unlike T_{LCST}, there appeared to be a difference in 2σ between QCM-D and SE measurements (Figure 3B). Except for the 52 nm thick film, the width associated with the SE measurements was similar to the bulk. The more narrow LCST associated with the QCM-D measurements may be an artifact of the unusual frequency response of the QCM-D at high swelling ratios as shown in Figure S8. Harmon, et al.[24] examined the width of the LCST in chemically crosslinked PNIPAAm and found the transition width to be about 0.5 ºC. The broad transition for NF5 is due to the physically crosslinked PNIPAAm and its distribution as described previously.[40]

In addition to thickness or mass, QCM-D can determine the viscoelastic properties of an adherent film that is sufficiently lossy. Figure 4 shows the temperature dependence of the shear viscosity (η) and shear elastic modulus (μ) of the hydrogel films calculated from the Voigt viscoelastic model[31] with frequency dependence.[44] The qualitative temperature dependence of η and μ is similar for all film thicknesses, but there are quantitative differences. For the thicker films (> 50 nm dry), both the viscosity and shear modulus were nearly

Soft Matter Accepted Manuscript

independent of thickness for temperatures below ~20 ºC, as shown in Figure 4. At low temperatures, η and μ were slightly lower for the 52 and 75 nm film than the thicker films, which was consistent with the greater extent of swelling (greater hydration) for the thinner films (Figure 1C). Consistent with the increased swelling for the 32 nm film, shear modulus and shear viscosity were significantly reduced at high swelling ratios. However, the data for the 10 nm film did not fall within the construct of the arguments proposed for the variation in viscoelastic properties for the thicker films. This film had the second largest swelling ratio of the films examined (Figure 1C), but the viscosity was greater than all of the films examined in the low temperature limit. We will return later to discuss the possible origins of this behaviour.

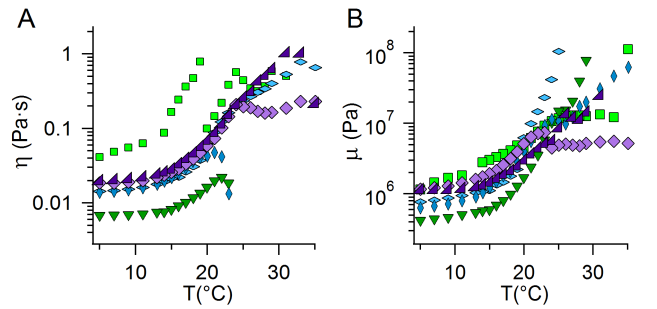

Figure 4. The viscoelastic properties of the hydrogels determined from QCM-D for the (**A**) viscosity and (**B**) shear elastic modulus as a function of temperature for the NF5 hydrogel films of dry thicknesses: 10 nm (■), 32 nm (▼), 52 nm (◂▸), 75 nm (♦), 100 nm (◆) and 120 nm (◢). At temperatures greater than 20-25 °C, the dissipation becomes sufficiently small that the viscoelastic properties cannot be accurately expressed by fitting of the QCM-D data as evidenced by the non-monotonic changes and large thickness variance especially for the shear elastic modulus.

At higher temperatures, there were significant variations in the viscoelastic properties for even the thicker films. The temperature dependence of η and μ seemed to vary erratically. This behavior was likely associated with low dissipation, which provides limited losses associated with the film by which the viscoelastic properties can be extracted. The fit of the high temperature data was not well constrained by the simple χ^2 error criteria for determining the best fit in Q-Tools. At high temperatures, the low dissipation values resulted in a wide range of satisfactory fits of the viscoelastic (Voigt) model to the frequency and dissipation data. That produced a large variance in the calculated viscoelastic properties of the film in the low dissipation regime as shown in the ESI (Part 6) for a 100 nm thick film. It is not clear why for some systems the viscoelastic properties was effectively modeled at low dissipation,[45] while for others issues such as shown here were encountered. For example, Patra and Toomey[46] reported high temperature η and μ calculated from QCM-D for photo-crosslinked PNIPAAm films, but they also reported difficulties in fitting their low dissipation data to the Voigt based viscoelastic model. Higher overtones were necessary and multiple thicknesses were fit simultaneously to the viscoelastic model in order to obtain the viscoelastic properties for the films.

The work by Patra and Toomey[46] for photo-crosslinked PNIPAAm films (36 - 144 nm) with a maximum volumetric swelling ratio of 2.6 provides an opportunity to compare the viscoelastic properties of chemically and physically crosslinked PNIPAAm. It should be noted that the swelling of these covalently crosslinked thin films was less than for the NF5 films examined here (3.9 - 4.9), but the expected swelling of an analogous bulk photo-crosslinked PNIPAAm is 6.8 (greater than the bulk NF5, 4.7). For the highly swollen state (low temperature), the viscosities of the thicker physically crosslinked (~0.02 Pa·s) and chemically crosslinked films (~0.04 Pa·s) were similar in comparison to the orders of magnitude changes that occurred as these hydrogels transversed across the LCST. The lower viscosity for NF5 is consistent with its larger swelling ratio in the highly swollen state. However when the NF5 was less swollen, near the onset of the effective viscoelastic modeling ($h/h_0 \sim 2$), the NF5 film viscosity was more than twice that of the fully collapsed covalently crosslinked PNIPAAm at high temperature. That behavior was unexpected since the water content in the NF5 was significantly greater than for the photo-crosslinked PNIPAAm films. Moreover, the shear modulus for the covalent network was consistently larger than that for NF5 films at similar water content, which may be related to the differences in the frequencies utilized in the viscoelastic model for fitting the QCM-D data.

Nonetheless, in both measurements the viscoelastic properties of the hydrogels were within approximately an order of magnitude of each other despite the small differences in the swelling ratios and nature of the crosslinks. This result further justifies the use of the 3rd and 5th overtones in fitting the QCM-D data, despite the upturn in frequency (Figure S8) for higher overtones. Additionally, frequency dependent exponents for both the viscosity and shear elastic modulus collapsed to similar values for all the films, except the 10 nm film as discussed in ESI (Part 7). At temperatures greater than 20 °C, the frequency dependence was highly variable. These temperatures correspond well with those where the primary viscoelastic properties were not consistently determined (Figure 4), which suggests that there is some dissipation limit at least for these NF5 hydrogels for effective fitting of the QCM-D data to a generalized model, which appears close to the Sauerbrey limit,[47] where the thickness can be accurately determined solely from the frequency change – i.e., neglecting viscoelasticity.

One anomaly in the calculated viscoelastic properties is related to the behavior of the 10 nm film, where the viscosity was larger than that of the other films. This behaviour is especially strange given that the swelling of that film was nearly the same as for the 32 nm film, which exhibited the lowest viscosity, determined by QCM-D, as would be expected for the largest swelling ratio. One possible explanation for the behavior of the 10 nm film is that the NF5 chains were strongly adsorbed to the substrate, which limited the mobility of the hydrogel. As the thickness of this film was initially commensurate with the size of the hydrophobic nanodomain crosslinks measured for a bulk hydrogel,[14] all of the chains may

Soft Matter Accepted Manuscript

 This journal is © The Royal Society of Chemistry 2012

be interacting with the substrate. Irreversible adsorption of polymer chains to substrates has been reported for other polymer systems,[28] so this adsorption to the substrate may account for the increase in viscosity of the thinnest hydrogel examined.

In general, these thin film hydrogels swell to bulk-like levels. It is proposed that an osmotic stress-induced rearrangement of the physical crosslinks[15, 48] provides a mechanism that enables this enhanced swelling of the thin films while still maintaining a stable gel network. The volumetric swelling ratio increased with decreasing film thickness, but the swelling constraint should be most prevalent nearest the substrate, so increased osmotic stress is expected. With increasing stress, the hydrophobic FOSA nanodomains are more prone to re-arrangement. Additionally despite the long time allowed for the films to equilibrate (~1 h) at each temperature step, careful examination of the plateau region of low temperature swelling curves for a single temperature step showed a slow increase in thickness for the thicker films after 60 min (see Figure S6). Thus, kinetic effects cannot be neglected for the apparent differences in swelling. That is, the rearrangement of the FOSA domains may be less hindered in the thin films and thus reach equilibrium in shorter time. It is useful to note that the low temperature swelling ratio was nearly identical for the 10 nm and 32 nm films, where this additional slow increase in thickness after 1 h was significantly reduced. Moreover, the swelling behavior is consistent with 1D Flory-Rehner at low swelling extents (high temperatures) where the imposed stress was low, but then significant deviations from that theory were observed at high swelling (low temperatures) for these physically crosslinked hydrogels, where the imposed stresses were significant. This behavior is consistent with the hypothesis of a reversible crosslink mechanism of stress-induced re-arrangements.

To further test this hypothesis of physical nanodomain rearrangement as the mechanism for the swelling enhanced in thin films compared with the Flory-Rehner predictions for crosslinked thin films, the swelling behavior through multiple heating/cooling cycles was examined. Stresses induced by swelling at low temperatures are hypothesized to induce breaking and re-forming of the physical network. From this rearrangement, it would be expected that significant hysteresis should be observed when cycling the film. Figure 5 illustrates the swelling behavior of a 32 nm film upon thermal cycling. The film was initially swollen as the temperature was decreased from 35 °C to 5 °C (denoted by 1 in Figure 5). Upon heating (denoted by 2 in Figure 5), the film did not contract to its initial swelling, consistent with our expectations based on re-arrangement of the physical crosslinks. Moreover, the swelling on subsequent cooling increases substantially. The swelling is significantly greater than that for the bulk hydrogel with the same chemical composition.

One plausible explanation for the hysteresis in swelling illustrated in Figure 5 relies on the mechanism for the determining the extent of the swelling of these hydrogels: the balance between osmotic stress and (anisotropic) chain stretching as well as the resistance of the physical crosslink to the imposed osmotic stress. This later consideration is not present for covalently crosslinked hydrogels as the strength of the covalent bond is much greater than the forces associated with the osmotic swelling. For the confined swelling in thin films, the unidirectional stress through the thickness of the film will be greater than that imposed by the isotropic swelling of the bulk hydrogel. This increased stress could enable re-arrangement of the FOSA domains, likely in an anisotropic manner due to confinement by the substrate, to enable additional swelling on re-cooling (denoted by 3 in Figure 5) that exceeds the swelling associated with the bulk hydrogel. An additional heating step (denoted by 4 in Figure 5) appears to faithfully follow the thicknesses associated with the prior cooling step as would be expected with no further re-arrangement of the network. Future work will focus on understanding the exact origins of this hysteresis and the associated nanostructure (FOSA domains) changes in these films as the material swells.

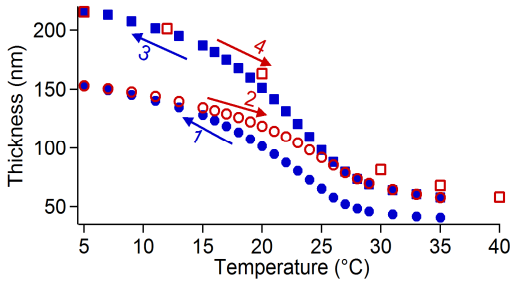

Figure 5. Temperature cycling for 32nm film. Blue filled symbols denote cooling, red open symbols denote heating. Circles are for first temperature cycling loop, squares are for second loop. The initial three cooling-heating-cooling (1-3) used 1-2 °C steps, while the final heating (4) used 5-10 °C steps. Significant hysteresis is consistent with film rearrangement, but the LCST remains almost uneffected.

With the ease in coating from solution without secondary crosslinking reactions and relative invariance in thermophysical properties with film thickness, these physically crosslinked and thermally responsive hydrogel coatings are promising candidates for thin responsive layers for biomedical and sensing applications.

Conclusions

The swelling behavior of a hydrophobically modified PNIPAAm hydrogel, NF5, was examined in thin films using QCM-D and SE. The volumetric swelling of these NF5 thin films is similar to that of the bulk hydrogel. We attribute this greater than expected swelling for the thin films to re-arrangement of the physical crosslinks due to osmotic stress. This flexibility in the network overcomes the conformational constraints typically associated with the substrate. This re-arrangement of the network leads to initial large hysteresis in the swelling on re-heating, but the second cooling-heating cycle appears to exhibit completely reversible behaviour with the volumetric swelling at low temperatures exceeding that of the bulk hydrogel. We attribute this behaviour to the anisotropic

Soft Matter Accepted Manuscript

nature of the swelling that provides directionality through the thickness of the film for the re-formation of the physical crosslinks based on FOSA domains. These results demonstrate that the physics associated with physically crosslinked hydrogel films differ significantly from those of the more commonly examined covalently crosslinked systems.

Acknowledgements

This work was partially supported by the Civil, Mechanical and Manufacturing Innovation Program (Directorate of Engineering) of the National Science Foundation, Grant CMMI 1300212. We acknowledge Jun Tian for the synthesis of the NF5 copolymer. We appreciate assistance with modeling of the QCM-D data from Mark Poggi and Archana Jaiswal (Q-Sense) and modeling of the SE data from Tom Tiwald, Greg Pribil, and Ron Synowicki (JA Woollam).

Notes and references

[a] Department of Polymer Engineering, University of Akron, Akron, OH 44313. vogt@uakron.edu (B.D.V.)

† Electronic Supplementary Information (ESI) available: This outlines the reasoning, implementation and justification for the temperature correction protocol used and developed for QCM-D measurement to account for thermo-physical changes of the bulk fluid and temperature effects inherent in the operation and use of the quartz sensor; the sigmoid fitting and explanation is provided for clarity; evidence of stress relaxation upon swelling is illustrated; demonstration of poor viscoelastic model results in low dissipative regime; and details of the frequency dependence modeling of the QCM-D data is explained. See DOI: 10.1039/b000000x/

1. I. Tokarev and S. Minko, *Soft Matter*, 2009, **5**, 511-524.
2. D. Puppi, F. Chiellini, A. M. Piras and E. Chiellini, *Progress in Polymer Science*, 2010, **35**, 403-440.
3. J. L. Drury and D. J. Mooney, *Biomaterials*, 2003, **24**, 4337-4351.
4. A. Richter, G. Paschew, S. Klatt, J. Lienig, K.-F. Arndt and H.-J. P. Adler, *Sensors*, 2008, **8**, 561-581.
5. A. C. Jen, M. C. Wake and A. G. Mikos, *Biotechnology and Bioengineering*, 1996, **50**, 357-364.
6. I. Tokarev and S. Minko, *Advanced Materials*, 2010, **22**, 3446-3462.
7. D. T. Eddington and D. J. Beebe, *Advanced Drug Delivery Reviews*, 2004, **56**, 199-210.
8. S. Chaterji, I. K. Kwon and K. Park, *Progress in Polymer Science*, 2007, **32**, 1083-1122.
9. P. Calvert, *Advanced Materials*, 2009, **21**, 743-756.
10. L. Y. Chu, Y. Li, J. H. Zhu and W. M. Chen, *Angewandte Chemie-International Edition*, 2005, **44**, 2124-2127.
11. T. Tanaka, *Physical Review Letters*, 1978, **40**, 820-823.
12. K. Dusek and Patterso.D, *Journal of Polymer Science Part a-2-Polymer Physics*, 1968, **6**, 1209-&.
13. P. Salehi, G. Makhoul, R. Roy, M. Malhotra, Z. A. Mood and S. J. Daniel, *Journal of Biomaterials Science-Polymer Edition*, 2013, **24**, 574-588.
14. J. Tian, T. A. P. Seery and R. A. Weiss, *Macromolecules*, 2004, **37**, 9994-10000.
15. J. K. Hao and R. A. Weiss, *Macromolecules*, 2011, **44**, 9390-9398.
16. S. S. Bae, K. Chakrabarty, T. A. P. Seery and R. A. Weiss, *Journal of Macromolecular Science-Pure and Applied Chemistry*, 1999, **A36**, 931-948.
17. T. L. Lowe, M. Benhaddou and H. Tenhu, *Journal of Polymer Science Part B-Polymer Physics*, 1998, **36**, 2141-2152.
18. C. W. Chen and M. Akashi, *Langmuir*, 1997, **13**, 6465-6472.
19. K. N. Plunkett, X. Zhu, J. S. Moore and D. E. Leckband, *Langmuir*, 2006, **22**, 4259-4266.
20. S. G. Lee, T. A. Pascal, W. Koh, G. F. Brunello, W. A. Goddard and S. S. Jang, *Journal of Physical Chemistry C*, 2012, **116**, 15974-15985.
21. B. C. Choi, S. Choi and D. E. Leckband, *Langmuir*, 2013, **29**, 5841-5850.
22. M. E. Harmon, D. Kuckling, P. Pareek and C. W. Frank, *Langmuir*, 2003, **19**, 10947-10956.
23. M. E. Harmon, D. Kuckling and C. W. Frank, *Macromolecules*, 2003, **36**, 162-172.
24. M. E. Harmon, T. A. M. Jakob, W. Knoll and C. W. Frank, *Macromolecules*, 2002, **35**, 5999-6004.
25. R. Toomey, D. Freidank and J. Ruhe, *Macromolecules*, 2004, **37**, 882-887.
26. P. J. Flory and J. Rehner, *The Journal of Chemical Physics*, 1943, **11**, 521-526.
27. E. L. Jablonski, V. M. Prabhu, S. Sambasivan, D. A. Fischer, E. K. Lin, D. L. Goldfarb, M. Angelopoulos and H. Ito, Conference on Advances in Resist Technology and Processing XXI, Santa Clara, CA, 2004.
28. S. Napolitano and M. Wubbenhorst, *Nature Communications*, 2011, **2**, 260.
29. T. A. P. Seery, M. Yassini, T. E. Hogenesch and E. J. Amis, *Macromolecules*, 1992, **25**, 4784-4791.
30. F. L. McCrackin, E. Passaglia, R. R. Stromberg and H. L. Steinberg, *Journal of Research of the National Institute of Standards and Technology*, 2001, **106**, 589-603.
31. M. V. Voinova, M. Rodahl, M. Jonson and B. Kasemo, *Physica Scripta*, 1999, **59**, 391-396.
32. J. J. I. Ramos, S. Stahl, R. P. Richter and S. E. Moya, *Macromolecules*, 2010, **43**, 9063-9070.
33. E. Reimhult, F. Hook and B. Kasemo, *Journal of Chemical Physics*, 2002, **117**, 7401-7404.
34. M. Rodahl, F. Hook, A. Krozer, P. Brzezinski and B. Kasemo, *Review of Scientific Instruments*, 1995, **66**, 3924-3930.
35. A.-L. Cauchy and C. d'analyse de l'Ecole, *Analyse Algébrique, V. París*, 1821.
36. M. Shibayama and T. Tanaka, *Advances in Polymer Science*, 1993, **109**, 1-62.
37. Q. Zhong, E. Metwalli, G. Kaune, M. Rawolle, A. M. Bivigou-Koumba, A. Laschewsky, C. M. Papadakis, R. Cubitt and P. Mueller-Buschbaum, *Soft Matter*, 2012, **8**.
38. C. H. Wang, S. Mukherjee, A. K. M. M. Islam, Y. W. Yang and M. Mukherjee, *Macromolecules*, 2011, **44**.
39. J.-F. Lutz, O. Akdemir and A. Hoth, *Journal of the American Chemical Society*, 2006, **128**.
40. J. Tian, T. A. P. Seery, D. L. Ho and R. A. Weiss, *Macromolecules*, 2004, **37**, 10001-10008.

Soft Matter Accepted Manuscript

 This journal is © The Royal Society of Chemistry 2012

41. B. D. Vogt, C. L. Soles, R. L. Jones, C. Y. Wang, E. K. Lin, W. L. Wu, S. K. Satija, D. L. Goldfarb and M. Angelopoulos, *Langmuir*, 2004, **20**, 5285-5290.
42. F. Hook, B. Kasemo, T. Nylander, C. Fant, K. Sott and H. Elwing, *Analytical Chemistry*, 2001, **73**, 5796-5804.
43. M. V. Voinova, M. Jonson and B. Kasemo, *Biosensors & Bioelectronics*, 2002, **17**, 835-841.
44. N. B. Eisele, F. I. Andersson, S. Frey and R. P. Richter, *Biomacromolecules*, 2012, **13**, 2322-2332.
45. S. W. Lee and D. Lee, *Macromolecules*, 2013, **46**, 2793-2799.
46. L. Patra and R. Toomey, *Langmuir*, 2010, **26**, 5202-5207.
47. C. C. White and J. L. Schrag, *Journal of Chemical Physics*, 1999, **111**, 11192-11206.
48. J. P. Gong, Y. Katsuyama, T. Kurokawa and Y. Osada, *Advanced Materials*, 2003, **15**, 1155-+.
49. C. A. Keller and B. Kasemo, *Biophysical Journal*, 1998, **75**, 1397-1402.
50. L. Macakova, E. Blomberg and P. M. Claesson, *Langmuir*, 2007, **23**, 12436-12444.

Soft Matter Accepted Manuscript